



HAL
open science

Analysis of Boundary-Layer Statistical Properties at Dome C, Antarctica

Jean-François Rysman, Sébastien Verrier, Alain Lahellec, Christophe Genthon

► **To cite this version:**

Jean-François Rysman, Sébastien Verrier, Alain Lahellec, Christophe Genthon. Analysis of Boundary-Layer Statistical Properties at Dome C, Antarctica. *Boundary-Layer Meteorology*, 2015, 156 (1), pp.145-155. 10.1007/s10546-015-0024-x . insu-01143166

HAL Id: insu-01143166

<https://insu.hal.science/insu-01143166>

Submitted on 14 Sep 2015

HAL is a multi-disciplinary open access archive for the deposit and dissemination of scientific research documents, whether they are published or not. The documents may come from teaching and research institutions in France or abroad, or from public or private research centers.

L'archive ouverte pluridisciplinaire **HAL**, est destinée au dépôt et à la diffusion de documents scientifiques de niveau recherche, publiés ou non, émanant des établissements d'enseignement et de recherche français ou étrangers, des laboratoires publics ou privés.

1 **Analysis of Boundary Layer Statistical Properties at**
2 **Dome C, Antarctica**

3 **Jean-François Rysman · Sébastien**
4 **Verrier · Alain Lahellec · Christophe**
5 **Genthon**

6 **Abstract** The boundary layer of the Antarctic Plateau is unique on account
7 of its isolated location and extreme stability. This study investigates the char-
8 acteristics of this boundary layer using wind and temperature measurements
9 from a 45-m high tower located at Dome C. First, spectral analysis reveals
10 that both fields have a scaling behaviour from 30 minutes to 10 days (spectral
11 slope $\beta \approx 2$). Wind and temperature time series also shows a multifractal
12 behaviour. Therefore, it is possible to fit the moment-scaling function to the
13 universal multifractal model and obtain multifractal parameters for temper-
14 ature ($\alpha \approx 1.51$ and $C_1 \approx 0.14$) and wind speed ($\alpha \approx 1.34$ and $C_1 \approx 0.13$).
15 The same analysis is repeated separately in winter and summer at six different
16 heights. The β parameter shows a strong stratification with height especially in

JF Rysman
UPMC Univ. Paris 06; Université Versailles St-Quentin; CNRS/INSU, LATMOS-IPSL,
France E-mail: jfrysman@lmd.polytechnique.fr

S Verrier
LOCEAN (UPMC/IPSL), CNES, France

A Lahellec
Laboratoire de Météorologie Dynamique, UPMC Univ. Paris 06, France

C Genthon
UJF - Grenoble 1 / CNRS Laboratoire de Glaciologie et Géophysique de l'Environnement
(LGGE), France

17 summer. This means that properties of turbulence change surprisingly rapidly
18 from the ground to the top of the tower.

19 **Keywords** Boundary Layer · Dome C · Meteorological tower · Scaling ·
20 Statistical properties

21 **1 Introduction**

22 The Antarctic surface consists of a plateau ranging from 2000 to 4000 m in
23 altitude and covered 98 % by ice (King and Turner, 1997). One of its local
24 maxima is Dome C (3233 m), where the Concordia station has been installed
25 since 1997. At this station, meteorological measurements are taken at the sur-
26 face with an automated weather station, while daily launched balloons pro-
27 vide soundings of the troposphere. As snow surface emissivity is higher than
28 atmosphere emissivity, significant temperature inversion exists in this region
29 at night and during winter (Hudson and Brandt, 2005; Genthon et al., 2013).
30 Moreover, surface winds are weak over the Eastern Antarctic Plateau where
31 the surface is smooth. These features, which inhibit turbulence and vertical
32 motions, explain the extremely stable boundary layer at Dome C. The bound-
33 ary layer may remain stable for several months almost without interruption,
34 leading to remarkable properties. The analysis of these properties is of high in-
35 terest to meteorologists since it provides the opportunity to better understand
36 the characteristics of an extremely stable boundary layer in an unperturbed
37 environment and facilitates the development of parameterizations aimed at
38 global and regional models.

39 Overall, boundary layer properties in Antarctica are poorly studied com-
40 pared with mid-latitude boundary layer properties because of the difficulty in
41 performing surface measurements. To fill this gap, a tower was installed in
42 2007 close to the Concordia station. Instruments were set up to measure wind,

43 temperature, and humidity at six levels along the 45 m tower. At present, this
44 is the highest tower that performs continuous measurements in Antarctica.
45 As the boundary layer depth in Antarctica is very shallow, the vertical vari-
46 ability is considerable and, for this reason, a tower is well adapted to study
47 boundary layer characteristics. The continuous measurements along the ver-
48 tical are particularly interesting when studying the boundary layer temporal
49 evolution and especially when analyzing the transition between the stable and
50 convective boundary layer that occurs on summer days.

51 In most Antarctic stations, except for the South Pole and Halley stations,
52 in-situ measurements are simply taken at standard meteorological levels (2
53 and 10 m). In addition, some measurement campaigns at high latitude regions
54 have been performed with an instrumented mast (e.g., King and Turner, 1997;
55 Travouillon et al., 2003; Grachev et al., 2005). As a result, long-term, in-situ,
56 and high-quality measurements of the low atmosphere at high latitude are
57 scarce and extremely valuable.

58 The present study is based on wind and temperature observations collected
59 from the tower at Dome C between January and December 2009. The objective
60 was to study the statistical properties of wind and temperature of the Dome C
61 boundary layer together with the vertical variability of these properties. The
62 analysis of the boundary layer is often difficult since processes with various
63 spatial and temporal scales occur conjointly. However, statistical properties
64 known as scaling or self-similarity can characterize this complex system with
65 only a few parameters. Experimental measurements have shown that scaling
66 properties are found in most geophysical fields and are related to atmospheric
67 turbulence, notably wind and temperature (Gage and Nastrom, 1986), cloud
68 radiance (Tessier et al., 1993), and rainfall (Verrier et al., 2011; Rysman et al.,
69 2013)). As a result, we chose to use this approach in this paper.

70 First, we highlight and analyze the scaling behaviour of wind and tem-
71 perature fields. In the second part of this analysis, we use the multifractal
72 framework to obtain parameters that describe the fields intrinsic properties.
73 This is the first time that such an innovative analysis is conducted in Antarc-
74 tica and for such an extremely stable boundary layer. This approach allows us
75 to characterize the full spectrum of signal variability that is not possible with
76 standard approaches.

77 **2 Data**

78 The Concordia scientific station is based on a local maxima called Dome C
79 ($75^{\circ} 06' \text{ S}$, $123^{\circ} 20' \text{ E}$, 3233 m a.s.l.) in the eastern part of the Antarctic
80 Plateau. The nearest coast is located more than 1000 km away. The local
81 slope of the Dome is about 5×10^{-4} toward the north and 1×10^{-3} toward the
82 east (based on NASA measurements at a 10' resolution). At this latitude, the
83 sun culminates at 38° on 21 December, and the winter night extends between
84 April and September.

85 In this study, we used meteorological instruments deployed along a 45 m
86 tower located 700 m from the Concordia station. The tower position was chosen
87 with respect to the atmospheric flow in order to minimize the influence of
88 station buildings. Six Vaisälä hygrometers (4 HMP155 and 2 HMP45AC),
89 six pt100 DIN IEC 751 thermistors, and six Young 45106 aero-vanes were
90 mounted at 3.6 m, 11 m, 18.6 m, 25.9 m, 33.2 m, and 42.4 m. Measurements
91 were performed with a 10-second time step and averaged over 30 minutes.
92 Additional technical details can be found in Genthon et al. (2010, 2013).

93 3 Methodology

94 3.1 Scaling

95 Initially, approaches based on a single exponent, called monofractal approaches,
 96 were used to characterize the scaling properties of a field over a given inertial
 97 range. Among these approaches, spectral analysis is widely used. It has been
 98 shown that if a physical field presents scaling properties, its power spectral
 99 density E (Priestley , 1981), proportional to the square of the modulus of the
 100 Fourier transform of the field, follows power-law behaviour as a function of
 101 frequency f (i.e., log-log linearity):

$$102 \quad E(f) \simeq f^{-\beta} \quad (1)$$

103 The β value depends on the correlation in a given field: a highly correlated
 104 field has a high β exponent, while a white noise (uncorrelated field) has a β
 105 exponent equal to zero (for details, see Rysman et al. (2013)).

106 Another way to highlight the scaling behaviour of a field is to test the first-
 107 order structure function log-log linearity. The first-order structure function
 108 corresponds to the statistical average of the absolute increments for different
 109 lags (this is a first-order function analogue to variograms):

$$110 \quad S(\delta t) = \langle |X(t + \delta t) - X(t)| \rangle \simeq \delta t^H \quad (2)$$

111 where δt is the time lag (varying from 0 to the time series length), S the first-
 112 order structure function and $\langle \rangle$ is the ensemble averaging operator. As for β ,
 113 H indicates the smoothness of the field.

114 3.2 Multifractal

115 Subsequently, refinements were proposed in order to take into account the
 116 strong inhomogeneity in the energy fluxes (e.g., Yaglom, 1966). These refine-
 117 ments rely on multiplicative cascades, that is, the representation of multiscale
 118 variability using a sequence of iterative multiplicative modulations of increas-
 119 ing resolution (e.g., Schertzer and Lovejoy, 1987; She and Leveque, 1994).
 120 Such models can usually be parameterized using a few exponents with more
 121 or less obvious physical interpretations, thus giving a description of a much
 122 wider class of variability than monofractal models (single parameter models).
 123 More precisely, multiplicative cascades generate multifractal stochastic fields.
 124 To investigate the validity of these theories with geophysical data, multifractal
 125 analysis procedures are applied (e.g., Verrier et al., 2011). The latter relies on
 126 the remarkable scaling properties of statistical moments of different orders that
 127 generalize the spectral scaling properties to a wider class of process intensities.

128 Statistically speaking, a field Φ follows multifractal properties if the statis-
 129 tical moments of the field depend on the resolution in a power-law manner. The
 130 power-law exponent only depends on the moment order, so that the statistical
 131 moments of the normalized field can be expressed as:

$$132 \quad \langle \Phi_\lambda^q \rangle \simeq \lambda^{K(q)} \quad (3)$$

133 where $\langle \rangle$ is the ensemble averaging operator, q the moment order (non-
 134 necessarily integer), λ the resolution, and $K(q)$ the moment-scaling function,
 135 which relates to scaling exponents and moments. In the following, the empirical
 136 statistical moments are denoted as $M_q(\lambda)$.

137 Several parameterizations of the fundamental moment-scaling function $K(q)$
 138 exist (e.g., Schertzer and Lovejoy, 1987; She and Leveque, 1994). In this pa-
 139 per, we consider the two-parameter universal form defined by Schertzer and

140 Lovejoy (1987). $K(q)$ is thus parametrized by two fundamental parameters,
 141 C_1 (intermittency parameter) and α (index of multifractality):

$$142 \quad K(q) = \frac{C_1}{\alpha - 1}(q^\alpha - q) \quad (4)$$

143 where $\alpha \in [0 : 2]$ and $\alpha \neq 1$ and $C_1 \in [0 : D]$ with D the dimension of the
 144 Euclidean space in which the field is defined (i.e., 1 in the case of time series).

145 A physical understanding of these parameters allows a given geophysical
 146 field to be characterized. C_1 can be related to the intermittency of the data,
 147 that is, the uniformity of the data around the mean. It increases as most of the
 148 measured values depart from the mean. α relates to the presence of extreme
 149 fluctuations within the field. High values of α indicate a field with a few large
 150 singularities (for details on the interpretation of multifractal parameters, see
 151 Pecknold et al., 1993; Purdy et al., 2001; Nykanen, 2008).

152 Often, Φ cannot be directly related to geophysical fields, because most of
 153 these fields and atmospheric processes are better described as low-pass filtered
 154 versions of multiplicative cascades. Therefore, a scaling filter such as fractional
 155 integration is usually applied (Schertzer and Lovejoy, 1987). Consequently,
 156 the properties of the conservative multifractal field Φ should be distinguished
 157 from the (usually) non-conservative integrated fields (the term integrated is
 158 related to the fractional integration needed to transform a conservative (non
 159 integrated) multifractal field to a realistic physical field (non conservative and
 160 integrated)).

161 The first step of a multifractal analysis is to determine whether the studied
 162 field is integrated. To this end, we use spectral analysis: if a field is integrated,
 163 its spectral slope is strictly (and notably) greater than 1. We then use the
 164 structure function. Indeed, the H exponent gives the order of fractional inte-
 165 gration in the field and physically represents the degree of smoothing involved

166 with the integration. For instance, $H = 0$ is associated with a conservative
 167 cascade (for details, see de Montera et al., 2009).

168 4 Results

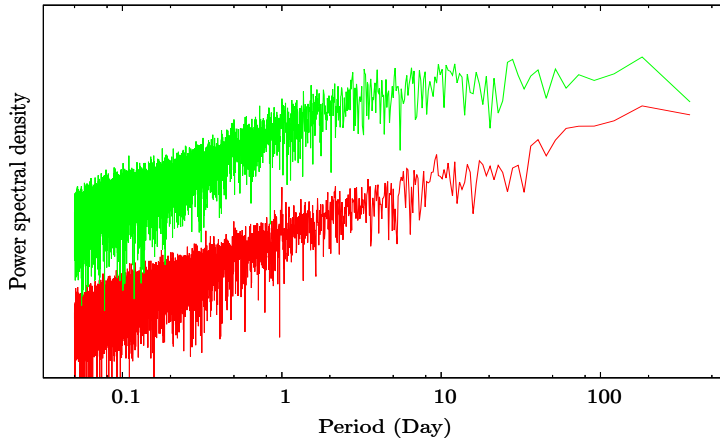


Fig. 1 Power spectral density of temperature ($\text{K}^2 \text{s}^{-1}$, red line) and zonal wind ($\text{m}^2 \text{s}^{-3}$, green line) at 42.4 m in a log-log plot

169 Figure 1 reveals that the power spectral density of zonal wind and temper-
 170 ature scale with a slope of respectively 2.20 and 2.02 at 42.4 m (from 2 hours
 171 up to 10 days). In other words, a high temporal autocorrelation exists be-
 172 tween these fields, with the temperature at a given time being related to the
 173 temperature up to 10 days later. For longer periods of time, both fields ap-
 174 pear uncorrelated (spectral slope equals zero) because the meteorological noise
 175 is greater than the remaining correlation. The region with periods exceeding
 176 10 days is often called the spectral plateau. The spectral plateau has been
 177 highlighted in various meteorological fields in the past (Fraedrich and Larn-
 178 der, 1993; Olsson, 1995; Fabry, 1996; Lovejoy and Schertzer, 2011; Rysman
 179 et al., 2013), with a decorrelation period ranging from 5 days to 1 month,
 180 which reveals a similarity among meteorological fields independent of local

181 characteristics. It must also be emphasized that both spectra are very similar
182 (similar slope and scaling range), suggesting a relationship between both vari-
183 ables. This similarity can be related to the influence of wind on temperature;
184 for example, when the wind changes direction, local temperature is affected.

185 Since spectral slopes greater than 1 are notably observed, it means that
186 the fields are integrated. The next step is to determine the degree of fractional
187 integration in the fields. Figure 2 shows the first-order structure functions of
188 the temperature and zonal wind series, averaged over height. Regarding tem-
189 perature, data only pertains to the period from January to October because
190 temperature sensors were interrupted for a few hours in October. For both
191 temperature and zonal wind, a scaling behaviour is found between 2 and 16 h
192 with an exponent H of about 0.69 (temperature) and 0.66 (zonal wind). This
193 confirms that for both variables, the observables should perhaps be related to
194 multifractal field only when applying a fractional integration. This is achieved
195 following Lavallée et al. (1993) and de Montera et al. (2009) with the compu-
196 tation of the absolute gradient of the time series.

197 The empirical moments of the latter are then estimated in order to confirm
198 the validity of Eq. 3. In a log-log plot, the multiscaling behaviour of moments
199 appears as a sequence of straight lines, each associated with a unique moment
200 order. Figure 3 shows the behaviour of statistical moments (between 0 and 2)
201 of temperature and zonal wind as a function of scale in log-log coordinates.
202 Two regimes thus appear: from 2 h to 2 days and from 2 days to 0.5 month. Red
203 lines at high frequencies show the fit of moment laws in the range 2 h-2 days.
204 In this range of scales, the moments (especially high-order moments) strongly
205 vary with the scale in a way that might be approximated by multifractal
206 laws. Larger scales are characterized by much slighter variations of moments,
207 represented by flat curves at low frequencies. This confirms the findings of
208 the structure function analysis above, wherein a scaling regime was found at

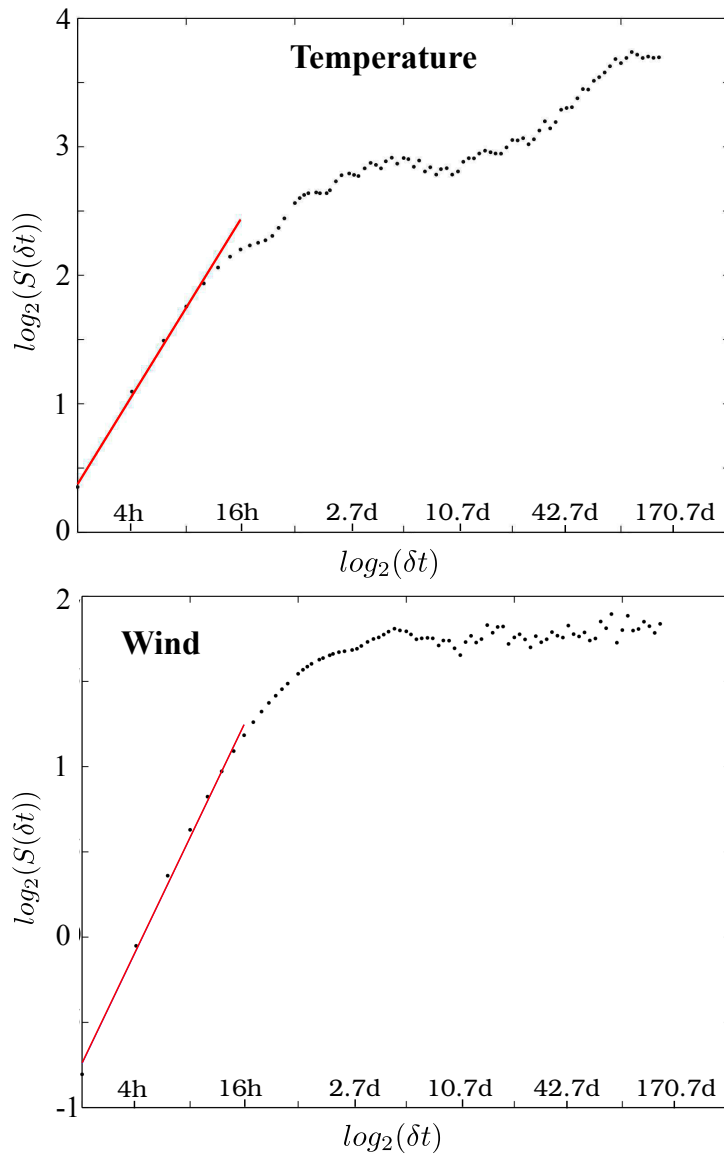


Fig. 2 First-order structure function ($S(\delta t)$) of temperature (K) and zonal wind (m.s⁻¹) averaged over heights as a function of time lag (δt) ranging from 2 h to 170.7 days. Linear regressions between 2 and 16 h are shown as red lines

209 high frequencies, while all statistics had more regular scale behaviour on larger
 210 scales.

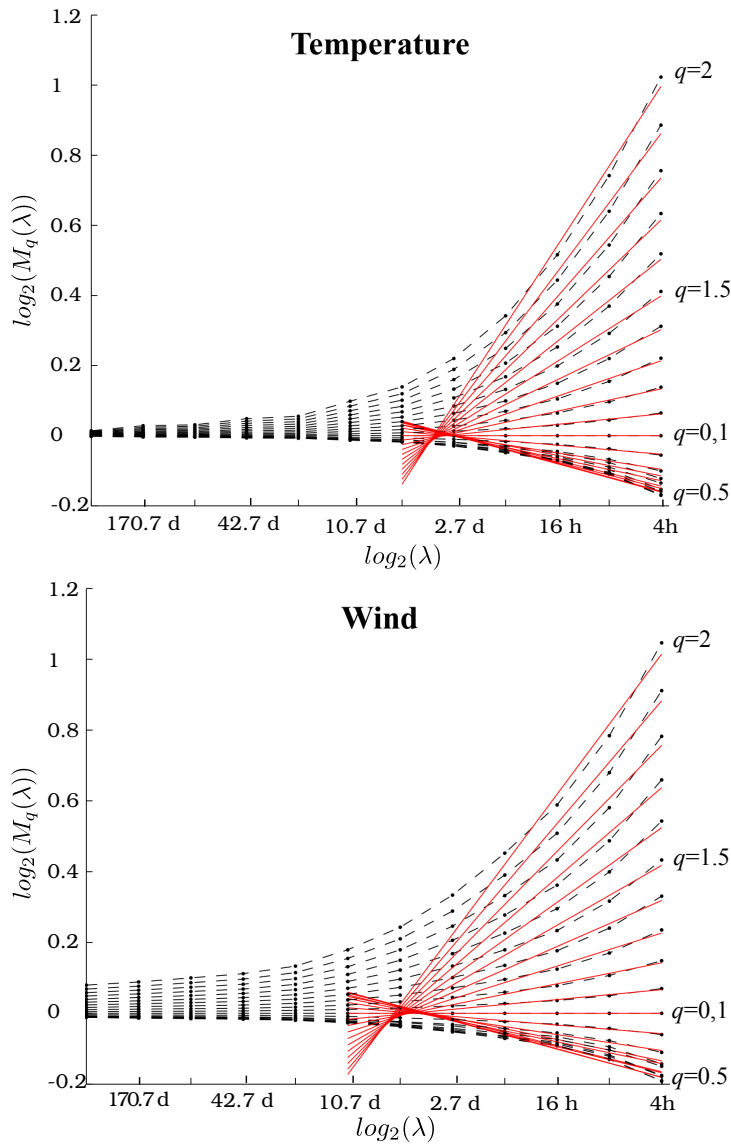


Fig. 3 Empirical moments ($M_q(\lambda)$) of the absolute temperature and zonal wind temporal gradients, averaged over heights as a function of the resolution ranging from 2 h to 170.7 days (log-log plot). Each straight line corresponds to a linear regression of the moments of fixed order q . The orders taken into consideration are $q = 0, 0.1, 0.2, \dots, 2.0$

211 Previous figures showed that zonal wind and temperature fields have mul-
 212 tifractal behaviour. The next step focusses on the multifractal parametrization
 213 of the 2 h-2 days regime in order to obtain C_1 and α parameters. Here, the

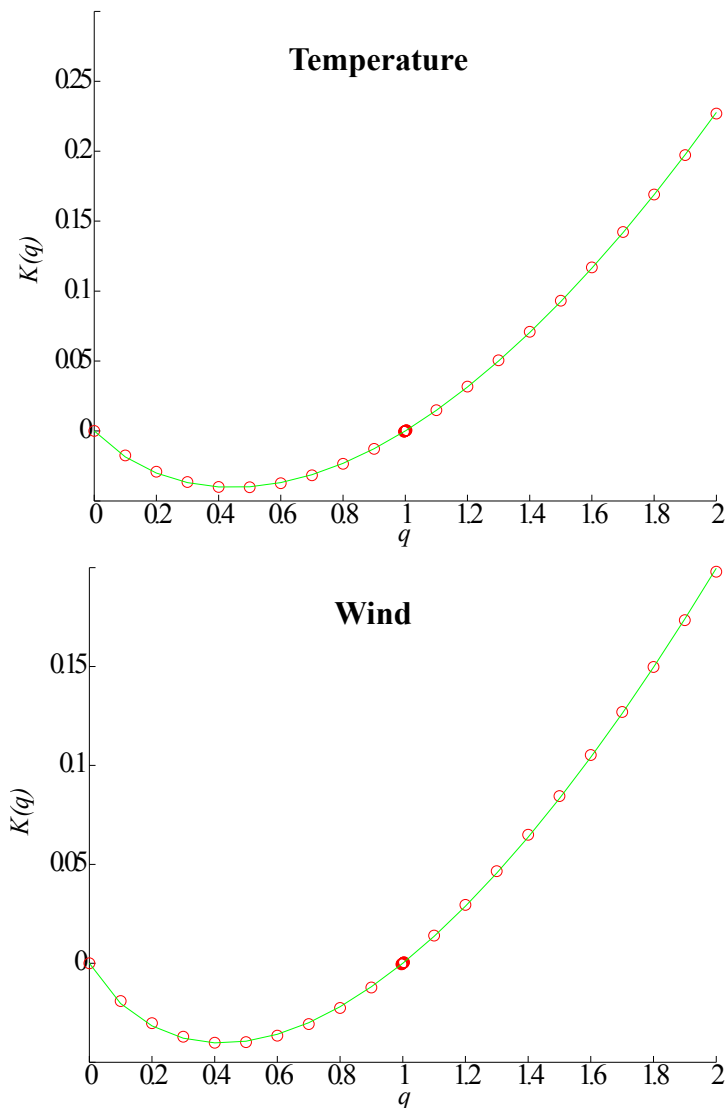


Fig. 4 Empirical moment-scaling function ($K(q)$) (red points), i.e., log-log slopes of the red fit lines in figure 3 and fit with universal multifractal model (green line) between 2 hours and 2 days for temperature and zonal wind averaged over height

214 slopes of the red fit lines previously computed are represented as a function
 215 $K(q)$ for moment order q (Figure 4). The curve of the empirical scaling ex-
 216 ponents $K(q)$ is superimposed to the least-square best fit of the universal (α ,
 217 C_1) form. First, we observe that the fits are very accurate, thus validating

218 the choice of parameterization proposed by Schertzer and Lovejoy (1987). The
219 best-fit parameters are $\alpha \approx 1.51$ and $C_1 \approx 0.14$ for temperature and $\alpha \approx 1.34$
220 and $C_1 \approx 0.13$ for zonal wind.

221 These parameters are consistent with previous multifractal analyses. For
222 instance, Schmitt et al. (1992) using laboratory observations obtained $\alpha \approx 1.2$
223 and $C_1 \approx 0.15$ for temperature and $\alpha \approx 1.3$ and $C_1 \approx 0.25$ for wind. Further,
224 Stolle et al. (2009); Lovejoy and Schertzer (2010); Stolle et al. (2012) using
225 model outputs from tropical and mid-latitude regions obtained, in average, for
226 wind and temperature $\alpha \approx 1.8$ and $C_1 \approx 0.12$. The most significant difference
227 is found for the α parameter, which is lower in our observations compared to
228 the model outputs in tropical and mid-latitude regions. This could indicate
229 that our observations have less extreme values. However, it is difficult to give
230 further interpretation because of the substantial differences between datasets.
231 Additional analysis and measurements are thus required in order to deter-
232 mine whether temperature and wind statistical properties significantly differ
233 at Dome C compared to other parts of the world.

234 Overall, the monofractal and multifractal results reveal the intrinsic quality
235 of the data. Indeed, positive slopes for spectra and moments highlight the
236 organisation (or correlation) within the geophysical field (see Nykanen, 2008;
237 Rysman et al., 2013), meaning that the noise of data is low compared to the
238 meteorological signal. Moreover, most of the fits show a rather low noise.

239 Turning to the effect of elevation and season on scaling parameters, the
240 same scaling analysis was applied separately to continuous period of summer
241 (January-February) and winter (July-August) seasons for each height (table
242 1).

243 Table 1 shows that scaling parameters depend on the season and height.
244 Overall parameters are lower during winter (e.g., for wind $\beta \simeq 2.00 \pm 0.03$)
245 than during summer (e.g., for wind $\beta \simeq 2.21 \pm 0.09$). Moreover, during winter,

Table 1 Multifractal parameters as a function of height and season (Summer (January-February) and Winter (July-August)). Missing data are indicated by a - and correspond to periods of interruptions for temperature sensors

Height (m)	Winter			
	Wind		Temperature	
	β	H	β	H
3.6	2.01±0.18	0.68±0.09	2.25±0.17	0.74±0.10
11	1.95±0.21	0.65±0.10	2.11±0.20	0.72±0.06
18.4	1.97±0.22	0.68±0.13	-	-
25.9	2.05±0.17	0.67±0.11	-	-
33.2	2.00±0.14	0.65±0.10	1.95±0.24	0.66±0.09
42.4	2.00±0.23	0.64±0.11	2.00±0.22	0.69±0.09
Summer				
3.6	2.06±0.17	0.68±0.05	2.14±0.22	0.91±0.03
11	2.14±0.14	0.72±0.04	2.05±0.23	0.85±0.06
18.4	2.22±0.13	0.75±0.04	1.89±0.28	0.75±0.07
25.9	2.26±0.12	0.74±0.04	1.91±0.17	0.71±0.06
33.2	2.28±0.14	0.75±0.04	1.92±0.18	0.69±0.05
42.4	2.29±0.13	0.75±0.04	1.89±0.23	0.68±0.06

246 β (2.00±0.03) and H (0.66±0.02) are rather constant with height for zonal
 247 wind while β and H decrease from the ground to the top of the tower for tem-
 248 perature (from 2.25 to 2 for β and from 0.74 to 0.69 for H). During summer,
 249 the zonal wind shows a stratification with height for the H (from 0.68 to 0.75)
 250 and the β parameters (2.06 to 2.29). Regarding temperature, H parameter
 251 goes from 0.91 to 0.68 and β goes from 2.14 to 1.89. The C_1 and α parameters
 252 do not seem to be affected by season or height for both fields (not shown in
 253 the table). Note that, as the uncertainties in β and H values are significant
 254 (see table 1), no definitive conclusions can be drawn on the significance of
 255 highlighted tendencies. Because boundary layer is almost continuously stable
 256 during winter, scaling parameters are characteristics of stable conditions dur-
 257 ing this season. During summer, boundary layer is alternatively convective and

258 stable. Therefore scaling parameters are likely to be affected by both stable
259 and convective conditions during this season.

260 5 Summary and Discussion

261 This study conducted an analysis of wind and temperature measurements
262 taken at Dome C during the 2009 field campaign. First, the computation of the
263 power spectra of wind and temperature reveals that both fields present scaling
264 properties from 30 minutes to 10 days with a β exponent of approximately 2.
265 Second, the analysis of the first-order structure function provides the degree
266 of fractional integration in both fields (i.e., $H= 0.69$ for temperature and
267 $H= 0.66$ for zonal wind). The computation of the empirical moment for the
268 temporal gradients of the wind and temperature time series reveals multifractal
269 behaviour. Thus, it is possible to use the universal multifractal model to fit
270 the moment-scaling function $K(q)$ and obtain the α and C_1 parameters. The
271 same analysis is repeated for winter and summer seasons for six elevations
272 and provides β and H parameters in these various conditions. While β and
273 H are constant with height during winter for the wind, a stratification of H
274 and β parameter is found during summer (e.g., from 2.06 to 2.29 for β). A
275 stratification of β and H parameter also exists for the temperature in both
276 winter and summer.

277 For the first time, this analysis provides scaling parameters in Antarctica
278 for a very stable boundary layer. An important result is the height depen-
279 dency for β and H especially in summer. For the zonal wind the parameters
280 increase from the ground to the top of the tower while for the temperature
281 the parameters decrease from the ground to the top of the tower. This result
282 is very surprising and to the authors best knowledge, this is the first time
283 that such an effect has been observed in these conditions. This behaviour is

284 probably related to the different properties of turbulence at the ground and at
285 the top of the tower due to the very strong temperature vertical gradient. In
286 particular, a steeper slope indicates a higher correlation within data; that is
287 turbulence could be stronger close to the ground than at higher levels. Further
288 interpretations require additional measurements of turbulence at Dome C.

289 This analysis could be used to evaluate parametrizations used in simula-
290 tions (Stolle et al., 2012, 2009). Indeed, many aspects of a meteorological field
291 can be fully characterized using the multifractal approach with only few coef-
292 ficients, e.g, the statistical moments and the probability distribution functions
293 of the field for scales ranging from the data resolution to the time series length.
294 Therefore, following the methodology of this paper, simulation outputs (and
295 associated parametrizations) could be evaluated in a new and innovative way.
296 In particular, this method could help to evaluate the statistical relationships
297 between scales in simulations (which is not usually done to our knowledge).
298 Moreover it will help identifying parametrizations that do not respect scaling-
299 laws i.e., that are not physically meaningful.

300 These computed values and our conclusions must be validated with other
301 measurements obtained in similar conditions, but to our knowledge, no previ-
302 ous scaling (including multifractal) analysis has been conducted in the region.
303 Finally, this analysis also highlights the intrinsic quality of our data. Indeed,
304 most of the fitted functions were found to have relatively little noise with
305 regard to the extreme atmospheric conditions. Since the tower still provides
306 data, it will be possible in the future to improve the accuracy of the scaling pa-
307 rameters. Moreover, measurements from sonic anemo-thermometers recently
308 deployed along the tower will be highly valuable to understand the scaling
309 properties of wind and temperature highlighted in this study.

310 **Acknowledgements** Boundary layer observation and research at Dome C were supported
311 by the French Polar Institute (IPEV; CALVA program), Institut National des Sciences
312 de l'Univers (Concordia and LEFE-CLAPA programs), and Observatoire des Sciences de
313 l'Univers de Grenoble (OSUG). We are grateful to Yvon Lemaître for his precious help. The
314 authors wish to thank two anonymous reviewers whose valuable feedback greatly improved
315 the manuscript.

316 **References**

- 317 de Montera L, Barthès L, Mallet C, Golé P (2009) The effect of rain-no rain
318 intermittency on the estimation of the universal multifractals model param-
319 eters. *J Hydrometeor* 10:493-506, DOI 10.1175/2008JHM1040.1
- 320 Fabry F (1996) On the determination of scale ranges for precipitation fields.
321 *J Geophys Res* 101:12,819–12,826, DOI 10.1029/96JD00718
- 322 Fraedrich K, Larnder C (1993) Scaling regimes of composite rainfall time series.
323 *Tellus A* 45(4):289–298
- 324 Gage KS, Nastrom GD (1986) Theoretical interpretation of atmospheric
325 wavenumber spectra of wind and temperature observed by commercial air-
326 craft during GASP. *J Atmos Sci* 43:729–740, DOI 10.1175/1520-0469
- 327 Genthon C, Town MS, Six D, Favier V, Argentini S, Pellegrini A (2010) Mete-
328 orological atmospheric boundary layer measurements and ECMWF analyses
329 during summer at Dome C, Antarctica. *J Geophys Res Atmos* 115:D05104,
330 DOI 10.1029/2009JD012741
- 331 Genthon C, Gallée H, Six D, Grigioni P, Pellegrini A (2013) Two years
332 of atmospheric boundary layer observation on a 45-m tower at Dome C
333 on the Antarctic plateau. *J Geophys Res Atmos* 118:3218–3232, DOI
334 10.1002/jgrd.50128
- 335 Grachev AA, Fairall CW, Persson POG, Andreas EL, Guest PS (2005) Stable
336 boundary-layer scaling regimes: the Sheba data. *Boundary-Layer Meteorol*

- 337 116:201–235, DOI 10.1007/s10546-004-2729-0
- 338 Hudson SR, Brandt RE (2005) A Look at the surface-based tempera-
339 ture inversion on the antarctic plateau *J Climate* 18:1673–1696, DOI
340 10.1175/JCLI3360.1
- 341 King JC, Turner J (1997) *Antarctic meteorology and climatology*. Cambridge
342 University Press, Cambridge
- 343 Lavallée D, Lovejoy S, Schertzer D, Ladoy P (1993) Nonlinear variability of
344 landscape topography: multifractal analysis and simulation. edited by L.
345 DeCola and N. Lam In: *Fractals and Geography*, Prentice Hall, New Jersey,
346 pp 158–192, 308 pp
- 347 Lovejoy S, Schertzer D (2010) Towards a new synthesis for atmospheric dy-
348 namics: Space-time cascades. *Atmos Res* 96:1–52
- 349 Lovejoy S, Schertzer D (2011) Space-time cascades and the scaling of ECMWF
350 reanalyses: Fluxes and fields. *J Geophys Res Atmos* 116:D14117, DOI
351 10.1029/2011JD015654
- 352 Nykanen DK (2008) Linkages between orographic forcing and the scaling prop-
353 erties of convective rainfall in mountainous regions. *J Hydrometeor* 9:327–
354 347, DOI 10.1175/2007JHM839.1
- 355 Olsson J (1995) Limits and characteristics of the multifractal behaviour of a
356 high-resolution rainfall time series. *Nonlinear Proc Geoph* 2:23–29
- 357 Pecknold S, Lovejoy S, Schertzer D, Hooge C, Malouin J (1993) The simu-
358 lation of universal multifractals. edited by J. M. Perdang and A. Lejeune
359 In: *Cellular Automata: Prospects in Astronomy and Astrophysics*, vol 1, pp
360 228–267 World Scientific, Hackensack, N. J., 416 pp
- 361 Priestley MB (1981) *Spectral analysis and time series*. Academic Press, New
362 York, 661 pp
- 363 Purdy JC, Harris D, Austin GL, Seed AW, Gray W (2001) A case study
364 of orographic rainfall processes incorporating multiscaling characterization

- 365 techniques. *J Geophys Res* 106:7837–7845, DOI 10.1029/2000JD900622
- 366 Rysman JF, Verrier S, Lemaître Y, Moreau E (2013) Space-time variability of
367 the rainfall over the western Mediterranean region: A statistical analysis. *J*
368 *Geophys Res Atmos* 118:8448–8459, DOI 10.1002/jgrd.50656
- 369 Schertzer D, Lovejoy S (1987) Physical modeling and analysis of rain and
370 clouds by anisotropic scaling multiplicative processes. *J Geophys Res*
371 92:9693–9714, DOI 10.1029/JD092iD08p09693
- 372 Schmitt F, Lovejoy S, Schertzer D, Lavallée D, Hooge C (1992) Estimations
373 directes des indices de multifractals universels dans le champ de vent et de
374 température. *C Rendues, de l’Acad Sciences (Paris)* 314:749–754
- 375 She Z, Leveque E (1994) Universal scaling laws in fully developed turbulence.
376 *Phys Rev Lett* 72:337–339
- 377 Stolle J, Lovejoy S, Schertzer D (2009) The stochastic multiplicative cascade
378 structure of deterministic numerical models of the atmosphere. *Nonlinear*
379 *Proc Geoph* 16:607–621
- 380 Stolle J, Lovejoy S, Schertzer D (2012) The temporal cascade structure of
381 reanalyses and global circulation models. *Q J R Meteorol Soc* 138:1895–
382 1913, DOI 10.1002/qj.1916
- 383 Tessier Y, Lovejoy S, Schertzer D (1993) Universal multifractals: theory and
384 observations for rain and clouds *Journal of Appl Meteor* 32:223–250, DOI
385 10.1175/1520-0450
- 386 Travouillon T, Ashley MCB, Burton MG, Storey JWV, Loewenstein RF (2003)
387 Atmospheric turbulence at the South Pole and its implications for astron-
388 omy. *Astron Astroph* 400:1163–1172, DOI 10.1051/0004-6361:20021814
- 389 Verrier S, Mallet C, Barthès L (2011) Multiscaling properties of rain in the
390 time domain, taking into account rain support biases. *J Geophys Res Atmos*
391 116:D20119, DOI 10.1029/2011JD015719

-
- 392 Yaglom AM (1966) The influence of fluctuations in energy dissipation on the
393 shape of turbulence characteristics in the inertial interval. Soviet Physics
394 Doklady 11:26–30